Electronic Supplementary Material (ESI) for ChemComm.

SUPPORTING INFORMATION

Symmetry Breaking Above Room Temperature in an Fe(II) Spin Crossover Complex with N_4O_2 Donor Set

Wasinee Phonsri,[a] Casey G. Davies,[b] Guy N. L. Jameson,[b]BoujemaaMoubaraki,[a] Jas S. Ward,[c] Paul E. Kruger,[c] Guillaume Chastanet,[d] and Keith S. Murray*[a]

[a] School of Chemistry, Monash University, Clayton, Victoria, 3800, Australia

[b] Department of Chemistry & MacDiarmid Institute for Advanced Materials and Nanotechnology, University of Otago, PO Box 56, Dunedin, 9054, New Zealand

[c] Department of Chemistry & MacDiarmid Institute for Advanced Materials and Nanotechnology, University of Canterbury, Private Bag 4800, Christchurch 8041, New Zealand.

[d]CNRS, Université de Bordeaux, ICMCB, 87 avenue du Dr. A. Schweitzer, Pessac 33608, France

Experimental Section

General: All reagents and solvents were purchased from Sigma–Aldrich and used as received. Infrared spectra were measured with a Bruker Equinox 55 FTIR spectrometer fitted with a 71Judson MCT detector and Specac Golden Gate diamond ATR. Mass spectrometry analyses were performed using electrospray ionization mass spectra (ESI-MS) and were recorded with a Micromass (now Waters) ZMD with Waters alliance e2695 HPLC system for automatic sample injections. MeOH was the mobile phase and had a flow rate of 100 μL min^{-1}. TGA measurements were performed using a MettlerTGA/DSC 1 thermal analysis instrument at a heating rate of 2 °C min^{-1}. Microanalyses were performed by Campbell Microanalytical Laboratory, Department of Chemistry, University of Otago, Dunedin, New Zealand. Variable-temperature magnetic susceptibility data were collected using either a Quantum Design MPMS 5 superconducting quantum interference device (SQUID) magnetometer or a MPMS XL-7 SQUID magnetometer, with a scan speed of 10 K min^{-1} followed by a one minute wait after each temperature change. In cases in which steps were less than 10 K the target temperature was reached in less than 1 min; hence it takes longer to stabilise at the target temperature. X-ray powder diffraction patterns recorded with a Bruker D8 Advance powder diffractometer operating at Cu Kα wavelength (1.5418 Å), with samples mounted on a zero-background silicon single crystal stage. Scans were performed at room temperature in the 2θ range 5–55°.

Mössbauer spectra were recorded on a spectrometer from SEE Co. (Science Engineering & Education Co., MN) equipped with a closed cycle refrigerator system from Janis Research Co. and SHI (Sumitomo Heavy Industries Ltd.). Data were collected in constant acceleration mode in transmission geometry. The zero velocity of the Mössbauer spectra refers to the centroid of the room temperature spectrum of a 25 μm metallic iron foil. Analysis of the spectra was conducted using the WMOSS program (SEE Co, formerly WEB Research Co. Edina, MN).

X-ray crystallographic measurements were collected at the University of Canterbury on an Agilent Supernova dual source (Cu, Mo) diffractometer fitted with an Atlas detector. The crystal quality was checked at 298 K by mounting on a loop with paratone oil, then the oil manually removed and the crystal remounted on a glass fibre with a minimal amount of epoxy resin. Full collections were performed at 298 K, 312 K, 330 K, 308 K, 318 K and 100 K

in that order, with a ramp rate of 60 Kh^{-1} (1 $Kmin^{-1}$) for all changes of the temperature (with the exception of 298 K to 100 K, where 120 Kh^{-1} (2 $Kmin^{-1}$) was used). A relaxation period of 15 minutes (from the time the final temperature was reached) for each temperature studied was allowed. Collection of complete data required approximately 24 hours per sample. After the six full collections (and numerous unit cell studies), no degradation of the crystal was observed, either physically or experimentally. All collections were performed with 20/80 (inner/outer data) second exposure times (correlated frames, so effectively 10/40 second exposures) for consistency.

Photomagnetic measurements were performed using a 650 nm photo-diode coupled by means of an optical fibre to the cavity of a MPMS-5S Quantum Design SQUID magnetometer. The optical power at the sample surface was adjusted to prevent important warming of the sample. The compound consists of a thin layer. Its weight was obtained by comparison of the thermal spin crossover curve with that of a more accurately weighted sample of the same material. Our previously published standardized method for measuring LIESST data was followed[1]: After being slowly cooled at 10K, the sample in the low-spin state was irradiated and the change in magnetic susceptibility was followed. When the saturation point was reached the laser was switched off and the temperature increased at a rate of ~ 0.4 K min^{-1}. The magnetization was measured every 1 K. T(LIESST) was determined from the minimum of a $d\chi_M T/dT$ vs. T plot for the relaxation process.

The *T*(LIESST) curve was recorded (Figure 8).[1, 2] This curve recorded at a constant temperature scan rate of 0.4 K/min informs on the lifetime of the photo-induced metastable state. The relaxation temperature *T*(LIESST) is obtained by pointing the minimum of the $\delta\chi_M T/\delta T$ curve.

Synthesis of ligands

Hqsal-Cl was synthesized according to the literature method.[3]

Synthesis of complexes

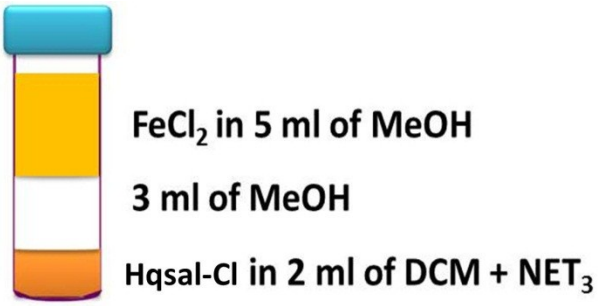

Layered diffusion is the general procedure that has been used to prepare the complexes. For the Fe(II) complex **1**: $FeCl_2 \cdot 4H_2O$ (40 mg, 0.2 mmol) was dissolved in MeOH (5 ml). The solution was stirred for 5 mins and then layered on to blank MeOH (3 ml). A solution of Hqsal-Cl (0.4 mmol) in CH_2Cl_2 (2 ml) was in the bottom in which NEt_3 (56 μL, 0.4 mmol) had been added as a base. After 7 days, black crystals formed, were washed with hexane (2 x 1 ml) and acetone (2 x 1 ml) and then air dried.

$[Fe(qsal\text{-}Cl)_2]$ yield 42 mg (34%). $\tilde{u}_{max}/cm^{-1}$:3043 ($\nu_{Ar\text{-}H}$), 1595 ($\upsilon_{C=N}$), 1562 ($\upsilon_{C=C}$), 1232 ($\upsilon_{C\text{-}N}$). m/z (ESI) 617.9 $[Fe(qsal\text{-}Cl)_2]^+$. Calcd. for (found%) $C_{32}H_{20}Cl_2FeN_4O_2$: C, 62.06 (61.21); H, 3.26 (3.14); N, 9.05% (8.92).

Table S1 Crystallographic data, CCDC numbers and structure refinement for iron(II) complex**1**

	100 K	**298 K**	**308 K**	**312 K**	**318 K**	**330 K**
Formula	$C_{32}H_{20}Cl_2FeN_4O_2$	$C_{32}H_{20}Cl_2FeN_4O_2$	$C_{32}H_{20}Cl_2FeN_4O_2$	$C_{32}H_{20}Cl_2FeN_4O_2$	$C_{32}H_{20}Cl_2FeN_4O_2$	$C_{32}H_{20}Cl_2FeN_4O_2$
Molecular weight / $gmol^{-1}$	619.27	619.27	619.27	619.27	619.27	619.27
Crystal system	Monoclinic	Monoclinic	Triclinic	Triclinic	Monoclinic	Monoclinic
Space group	$P2_1/n$	$P2_1/n$	$P\bar{1}$	$P\bar{1}$	$P2_1/n$	$P2_1/n$
a / Å	10.2044 (2)	10.2113 (2)	10.2926 (5)	10.3266 (6)	10.3632 (3)	10.3970 (4)
b / Å	12.8835 (2)	12.9889 (2)	13.0726 (5)	13.1023 (6)	13.1281 (3)	13.1513 (4)
c / Å	19.3776 (4)	19.6876 (4)	19.6371 (8)	19.6014 (9)	19.5466 (5)	19.5205 (6)
α / °	90	90	90.988 (3)	90.696 (4)	90	90
β / °	93.6752 (18)	93.2672 (18)	93.801 (3)	93.869 (4)	94.034 (3)	94.140 (3)
γ / °	90	90	90.596 (3)	90.429 (4)	90	90
Cell volume / $Å^3$	2542.30 (9)	2606.99 (9)	2635.81 (19)	2645.8 (2)	2652.71 (12)	2662.15 (15)
Z	4	4	4	4	4	4
Reflections collected	17188	18456	19835	20178	19430	19362
Independent reflections, R_{int}	5085, 0.0477	5228, 0.0436	10745, 0.0424	10788, 0.0518	5512, 0.0458	5544, 0.0501
Restraints/parameters	0/370	0/370	0/739	0/739	0/370	0/370
Final R indices [$I>2\sigma(I)$]: R_1, wR_2	0.0437, 0.1186	0.0436, 0.1215	0.0655, 0.2002	0.0673, 0.2083	0.0452, 0.1314	0.0483, 0.1431
CCDC No.	1495808	1495809	1495810	1495811	1495812	1495813

Table S 2 Selected bond length and octahedral distortion parameters for **1**

	100 K	**298 K**	**308 K**	**312 K**	**318 K**	**330 K**
Fe1-O1/Å	1.9553 (16)	1.9632 (18)	1.968 (3)	1.979 (3)	1.996 (2)	2.005 (2)
Fe1-O2/Å	1.9590 (17)	1.961 (2)	1.954 (4)	1.969 (4)	2.004 (3)	2.013 (3)
Fe1-N1/Å	1.939 (2)	1.961 (2)	2.001 (3)	2.029 (3)	2.096 (2)	2.113 (2)
Fe1-N2 /Å	1.9491 (19)	1.983 (2)	2.028 (3)	2.066 (4)	2.128 (2)	2.158 (2)
Fe1-N3/Å	1.956 (2)	1.962 (2)	1.995 (3)	2.028 (4)	2.089 (2)	2.112 (2)
Fe1-N4 /Å	1.937 (2)	1.989 (2)	2.030 (3)	2.066 (4)	2.131 (2)	2.158 (3)
Fe51-O51/Å			1.993 (3)	2.006 (3)		
Fe51-O52/Å			2.005 (4)	2.007 (4)		
Fe51-N51/Å			2.085 (3)	2.090 (4)		
Fe51-N52 /Å			2.133 (3)	2.139 (3)		
Fe51-N53/Å			2.089 (3)	2.096 (4)		
Fe51-N54 /Å			2.131 (4)	2.138 (4)		
Σ/° (Fe1, Fe51)	34	32	38, 61	45, 63	62	69
Θ/° (Fe1, Fe51)	65	74	94, 176	119, 184	178	199

Table S 3 Intermolecular interactions in [Fe(qsal-Cl)$_2$] **1**

	100 K	298 K	308 K	312 K	318 K	330 K
A chain along *b* axis						
π-π	3.304	3.352	3.386	3.406	3.427	3.436
π-π	3.213	3.258	3.282	3.307	3.312	3.330
C9-H9···O2	2.4323(0)	2.4739(0)	2.4784(1)	2.4460(1)	2.4653(0)	2.4701(1)
C23-H23···O1	2.6129(0)	2.6624(0)	2.6750(1)	2.6718(1)	2.7078(1)	2.7174(1)
C21-H21···O1	2.8901(0)	2.9855(0)	2.9405(1)	2.8553(1)	2.7773(1)	2.7437(1)
π-π			3.414	3.416		
π-π			3.292	3.301		
C59-H59···O52			2.4600(1)	2.3392(1)		
C73-H73···O51			2.7077(1)	2.6771(1)		
A chain along *c* axis						
C2-H2···Cl1 Van Der Waals Radius H =1.2, Cl = 1.75Å	[2.9594(0)]	[3.041(0)]	[3.0476(1)(Cl1-H52)]	[3.0553(1)(Cl1-H52)]	[2.9972(1)]	[2.9944(1)]
π-π	3.296	3.360	3.450(C19-C80)	3.478(C19-C80)	3.489	3.512
π-π	3.349	3.431	3.559(C3-C64)	3.568(C3-C64)	3.560	3.587
A chain along *a* axis						
P4AE1						
π-π	3.555	3.598	3.610	3.562	3.486	3.471
C26-H26···π	2.850	2.964	2.830	3.001	3.016	3.084
P4AE2						
π-π	3.556	3.594	3.625	3.615	3.596	3.597
C11-H11···π	2.664	2.727	2.580	2.754	2.749	2.844
P4AE51						
π-π			3.470	3.475		
C76-H76···π			3.005	3.121		
P4AE52						
π-π			3.569	3.578		
C61-H61···π			2.680	2.741		
C18-H18···Cl2	2.8334(0)	2.9045(0)	2.9177(1)(Cl2-H68) 2.7889(1)(Cl52-H18)	2.8865(1)(Cl2-H68) 2.7763(1)(Cl52-H18)	2.8113(1)	2.8021(1))

Table S 4 Review of two-step SCO with symmetry breaking

Fe centre	Compound[a]	Coordination Environment	Type of SCO[b]	$T_{1/2}$/K(heat)	Ref
2+	$[Fe(L^{16})_2](ClO_4)_2$	N_6	G	170, 245	4
	$[Fe(Hpy\text{-}DAPP)](BF_4)_2$	N_6	G	140, 190	5
	$[\{Fe^{II}(NCBH_3)(4phpy)\}_2(\mu\text{-}bpypz)_2]$	N_6	G	160, 220	6
	$[Fe(H_2L^{2\text{-}Me})_2]Br{\cdot}ClO_4{\cdot}0.5EtOH$	N_6	G	110, 220	7
	$[FeH_2L^{2\text{-}Me}][AsF_6]_2$	N_6	G	≈100, 150	8
	$[FeH_2L^{2Me}](PF_6)_2$	N_6	G	97, 150	9
	$[Fe(2\text{-}pic)_3]Cl_2{\cdot}EtOH$	N_6	A	114, 124	10
	$[Fe(3\text{-}Clpy)_2Pd(CN)_4]$	N_6	A	148, 164	11
	$[FeH_3L^{Me}]Cl{\cdot}AsF_6$	N_6	A	82, 122	12
	$[Fe(5\text{-}NO_2\text{-}sal\text{-}N(1,4,7,10))]$	N_4O_2 (hexadentate)	A	136, 171	13
	$[Fe(bpmen)(NCSe)_2]$	N_6	A	106, 120	14
	$[Fe(bapbpy)(NCS)_2]$	N_6	A	194, 239	15
	$[Fe(bdpt)_2]{\cdot}EtOH$	N_6	A	121, 158	16
	$[Fe(bdpt)_2]{\cdot}MeOH$	N_6	A	128, 176	16
	$[Fe(bdpt)_2]$	N_6	A	144, 192	16
3+	$[Fe(nsal_2trien)]SCN$	N_4O_2	G	124, 250	17
	[Fe(salpm)2]ClO4·0.5EtOH	N_4O_2	A	115, 171	18
	$[Fe(qsal\text{-}Br)_2]NO_3{\cdot}2MeOH$	N_4O_2	A	136, 232	19

[a] Only complete two step spin crossover for Fe mononuclear system[b]A = abrupt and G = gradual

L^{16} = 2-(2-n-Hexadecyl-2H-etrazol-5-yl)-1,10-phenanthroline, Hpy-DAPP = bis[*N*-(2-pyridylmethyl)-3-aminopropyl](2-pyridylmethyl)amine, 4phpy = 4-phenylpyridine, Hbpypz = 3,5-bis(2-pyridyl)-pyrazole, $H_2L^{2\text{-}Me}$ =methylimidazol-4-yl-methylidenehistamine ($[Fe(H_2L^{2\text{-}Me})_2]Br{\cdot}ClO_4{\cdot}0.5EtOH$), $H_2L^{2\text{-}Me}$ = bis{[(2-methylimidazol-4-yl)methylidene]-3-aminopropylethylenediamine. ($[FeH_2L^{2\text{-}Me}][AsF_6]_2$), H_2L^{2Me} = bis[N-(2-methylimidazol-4-yl)methylidene-3-aminopropyl]ethylenediamine, 2-pic = 2-picolylamine, H_3L^{Me} = Tris[2-(((2-methylimidazol-4-yl)methylidene)amino)ethyl]amine), bpmen = N,N'-dimethyl-N,N'-bis(2-pyridylmethyl)-1,2-ethanediamine, bapbpy = *N*-(6-(6-(pyridin-2-ylamino)pyridin-2-yl)pyridin-2-yl)pyridin-2-amineHbdpt = 3-(5-bromo-2-pyridyl)-5-(4-pyridyl)-1,2,4-triazole)

NB For a recent review see Ortega-Villar et al., *Magnetochemistry* 2016[20]

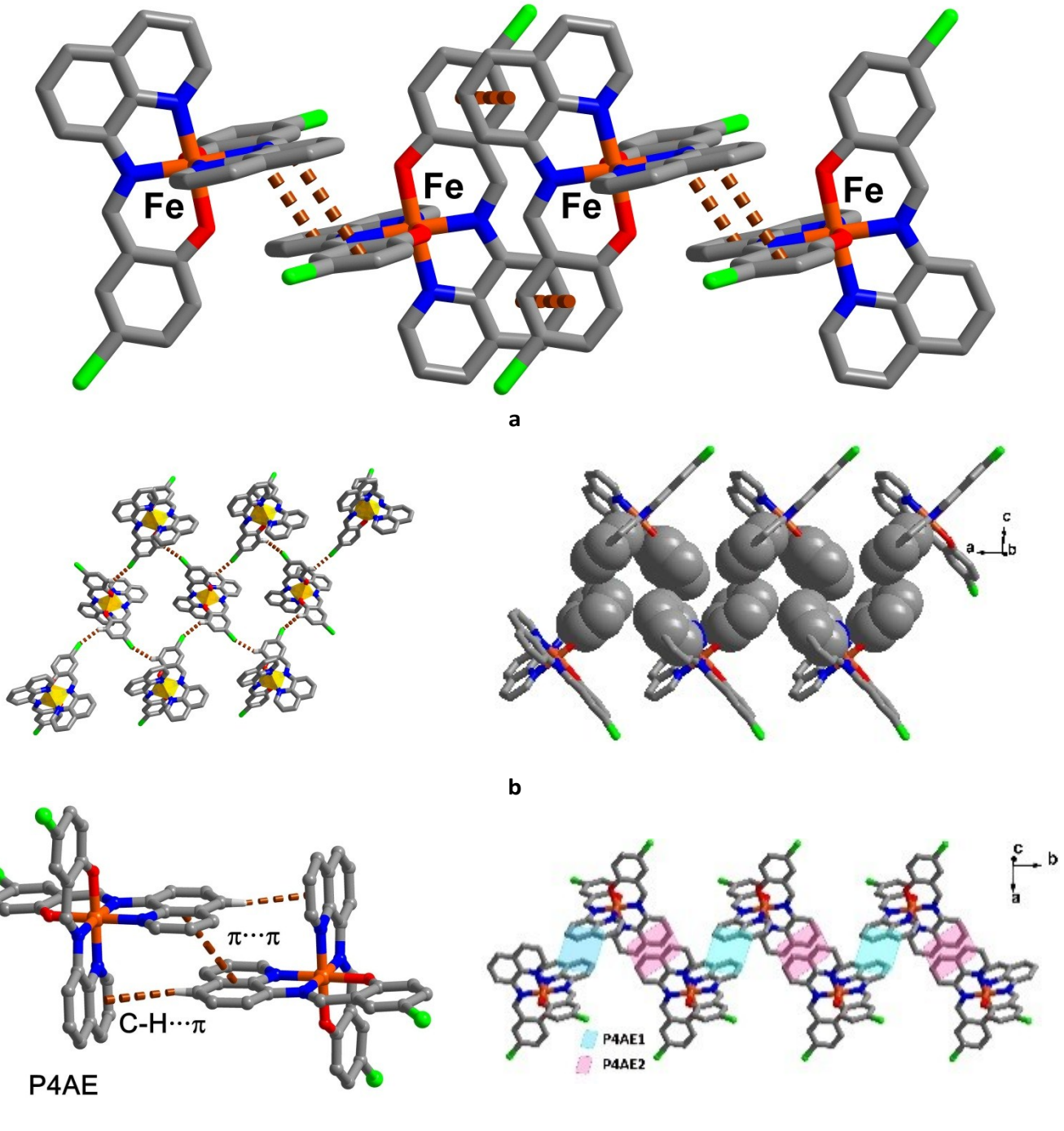

Fig S 1 Representations of a) π-π interactions connecting Fe complex molecules into a chain. b) C-H···Cl and π-π interactions connecting in a plane along the c axis. c) two sets of P4AE interactions present in **1**

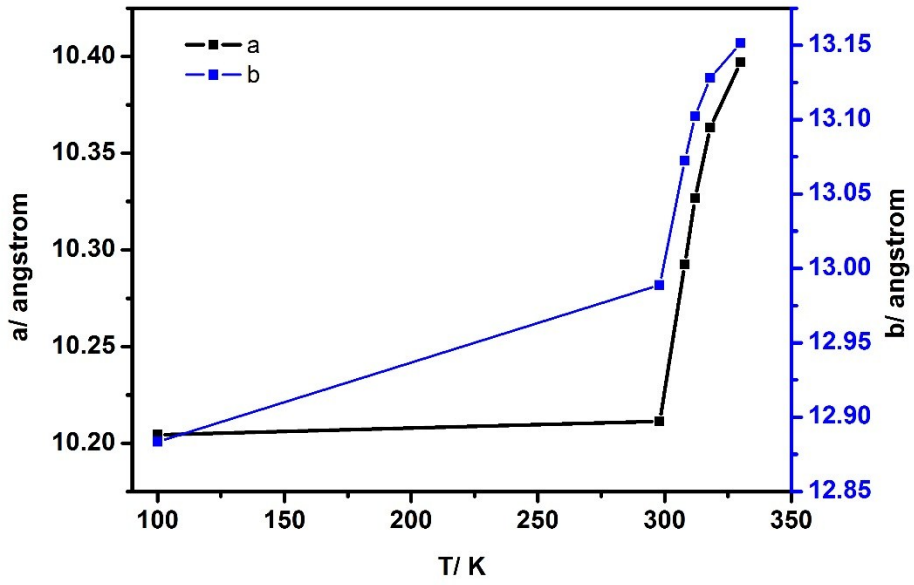

a

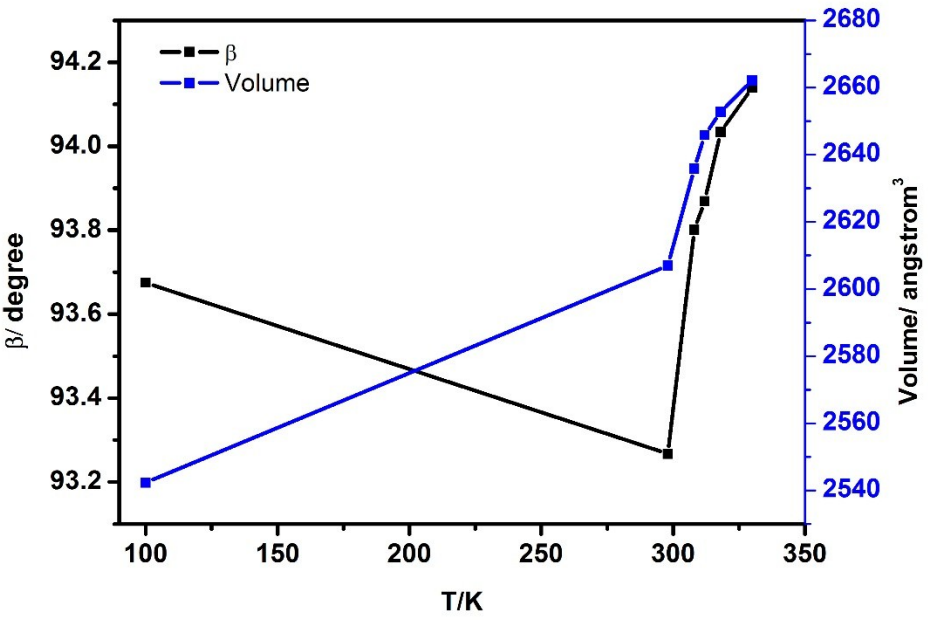

b

Fig S 2 The unit cell parameters of variable-temperature structures of **1** vs. temperature for a) *a* and *b* parameters and b) *β* angle and volume of the unit cell

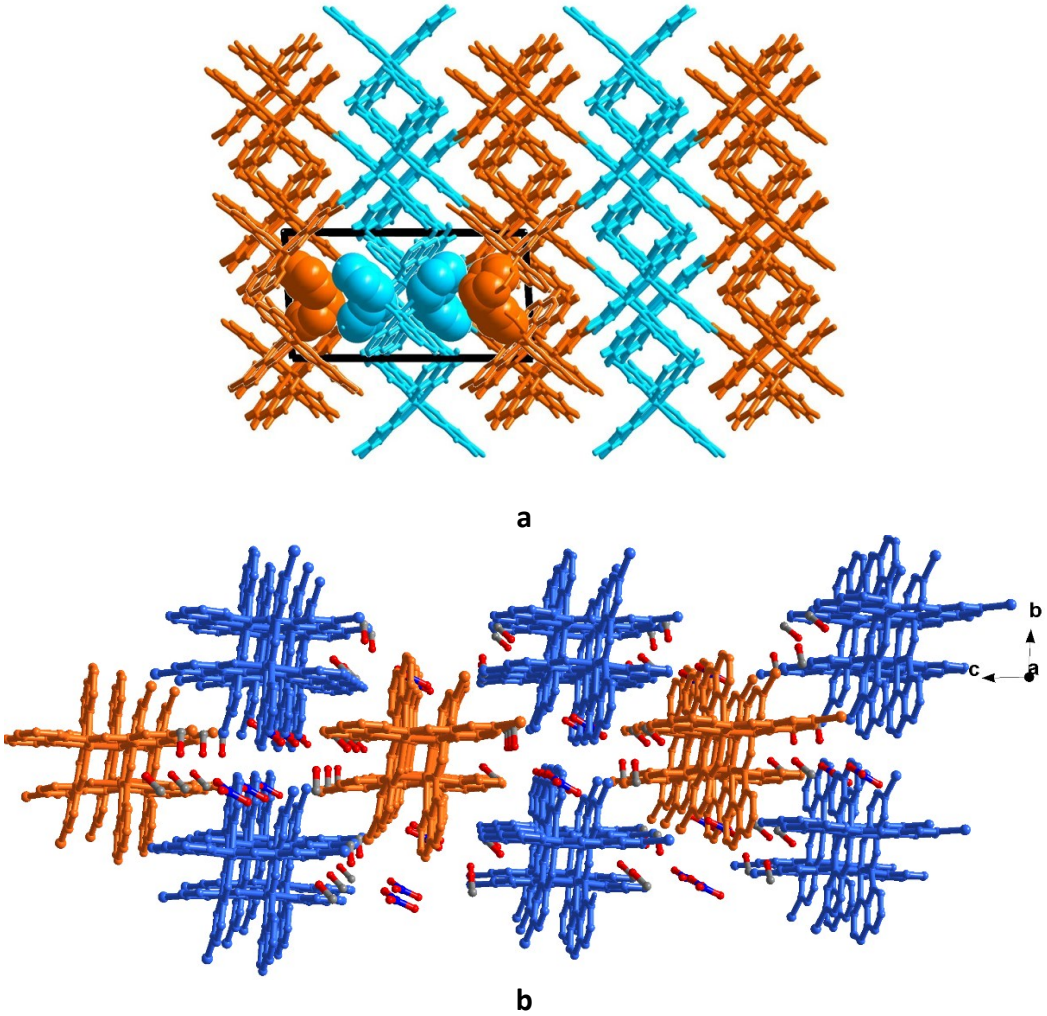

Fig S 3 The packing of intermediate phases of a) **1**at 308 K and b) $[Fe(qsal\text{-}Br)_2]NO_3 \cdot 2MeOH$[19] at 175 K (blue is LS, orange is HS)

Table S 5 ^{57}Fe Mössbauer spectral parameters for**1**

Compound	T (K)	Spin State	δ (mm/s)	ΔE_Q (mm/s)	$\Gamma_{L/R}$ (mm/s)	I (%)
1	5.9	LS	0.43	1.09	0.27/0.24	100
	295	LS	0.34	1.03	0.36	90
		HS	1.20[a]	1.87	0.27/0.65	10

[a] Strong evidence for HS Fe(II) but unable to fit unambiguously.

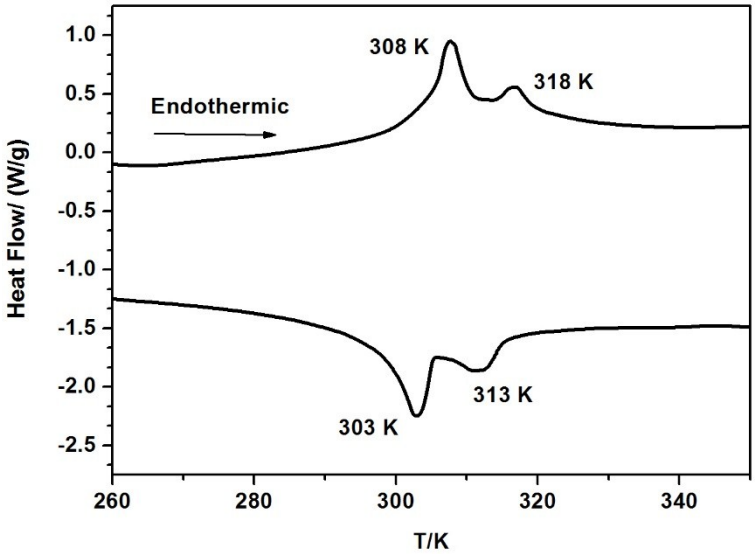

Fig S 4 DSC plots for compound **1**

Table S 6 Calculated ΔH and ΔS from DSC results of the compound**1**.

ΔH/J/mol		**ΔS/ J/molK**	
Endo	**Exo**	**Endo**	**Exo**
5.7	6.0	18.5	19.8

References

1. J.-F. Létard, L. Capes, G. Chastanet, N. Moliner, S. Létard, J.-A. Real and O. Kahn, *Chem. Phys. Lett.*, 1999, **313**, 115-120.
2. J.-F. Létard, G. Chastanet, P. Guionneau and C. Desplanches, in *Spin-Crossover Materials*, John Wiley & Sons Ltd, 2013, DOI: 10.1002/9781118519301.ch19, pp. 475-506.
3. J. Sirirak, W. Phonsri, D. J. Harding, P. Harding, P. Phommon, W. Chaoprasa, R. M. Hendry, T. M. Roseveare and H. Adams, *J. Mol. Struct.*, 2013, **1036**, 439-446.
4. W. Zhang, F. Zhao, T. Liu, M. Yuan, Z.-M. Wang and S. Gao, *Inorg. Chem.*, 2007, **46**, 2541-2555.
5. M. Buron-Le Cointe, N. Ould Moussa, E. Trzop, A. Moréac, G. Molnar, L. Toupet, A. Bousseksou, J. F. Létard and G. S. Matouzenko, *Phys. Rev. B*, 2010, **82**, 214106.
6. K. Nakano, S. Kawata, K. Yoneda, A. Fuyuhiro, T. Yagi, S. Nasu, S. Morimoto and S. Kaizaki, *Chem. Commun.*, 2004, 2892-2893.
7. T. Sato, K. Nishi, S. Iijima, M. Kojima and N. Matsumoto, *Inorg. Chem.*, 2009, **48**, 7211-7229.
8. N. Bréfuel, E. Collet, H. Watanabe, M. Kojima, N. Matsumoto, L. Toupet, K. Tanaka and J.-P. Tuchagues, *Chem. Eur. J.*, 2010, **16**, 14060-14068.
9. N. Bréfuel , H. Watanabe, L. Toupet, J. Come, N. Matsumoto, E. Collet, K. Tanaka and J.-P. Tuchagues, *Angew. Chem. Int. Ed.*, 2009, **48**, 9304-9307.
10. D. Chernyshov, M. Hostettler, K. W. Törnroos and H.-B. Bürgi, *Angew. Chem. Int. Ed.*, 2003, **42**, 3825-3830.
11. V. Martínez, Z. Arcís Castillo, M. C. Muñoz, A. B. Gaspar, C. Etrillard, J.-F. Létard, S. A. Terekhov, G. V. Bukin, G. Levchenko and J. A. Real, *Eur. J. Inorg. Chem.*, 2013, **2013**, 813-818.
12. M. Yamada, H. Hagiwara, H. Torigoe, N. Matsumoto, M. Kojima, F. Dahan, J.-P. Tuchagues, N. Re and S. Iijima, *Chem. Eur. J.*, 2006, **12**, 4536-4549.
13. D. Boinnard, A. Bousseksou, A. Dworkin, J. M. Savariault, F. Varret and J. P. Tuchagues, *Inorg. Chem.*, 1994, **33**, 271-281.
14. J. Luan, J. Zhou, Z. Liu, B. Zhu, H. Wang, X. Bao, W. Liu, M.-L. Tong, G. Peng, H. Peng, L. Salmon and A. Bousseksou, *Inorg. Chem.*, 2015, **54**, 5145-5147.
15. S. Bonnet, M. A. Siegler, J. S. Costa, G. Molnar, A. Bousseksou, A. L. Spek, P. Gamez and J. Reedijk, *Chem. Commun.*, 2008, 5619-5621.
16. J.-B. Lin, W. Xue, B.-Y. Wang, J. Tao, W.-X. Zhang, J.-P. Zhang and X.-M. Chen, *Inorg. Chem.*, 2012, **51**, 9423-9430.
17. B. J. C. Vieira, J. T. Coutinho, I. C. Santos, L. C. J. Pereira, J. C. Waerenborgh and V. da Gama, *Inorg. Chem.*, 2013, **52**, 3845-3850.
18. K. D. Murnaghan, C. Carbonera, L. Toupet, M. Griffin, M. M. Dîrtu, C. Desplanches, Y. Garcia, E. Collet, J.-F. Létard and G. G. Morgan, *Chem. Eur. J.* , 2014, **20**, 5613-5618.
19. D. J. Harding, W. Phonsri, P. Harding, K. S. Murray, B. Moubaraki and G. N. L. Jameson, *Dalton Trans.*, 2015, **44**, 15079-15082.
20. N. Ortega-Villar, M. Muñoz and J. Real, *Magnetochemistry*, 2016, **2**, 16.